TOPICAL REVIEW

Surface induced ordering effects in soft condensed matter systems

Peter Lang

Forschungszentrum Jülich, Institut für Festkörperforschung, 52425 Jülich, Germany

E-mail: p.lang@fz-juelich.de

Abstract
The symmetry break of the particle interaction field at surfaces causes a variety
of interfacial effects including the variation of the relative stability of different
phases of a given compound. In many materials surface melting is observed,
i.e. a surface near a portion of the system is in a less ordered state than the bulk.
Over the last two decades, surface ordering, i.e. the stabilization of the higher
ordered phase by the surface, has been observed for an increasing number of soft
condensed matter systems. For melts of low molar mass compounds, surface
freezing has been reported so far only for chain molecules, while in systems
of colloidal length scale, surface ordering has been observed for spherical
particles as well. In this contribution we will review experimental studies, some
theoretical approaches as well as computer simulations of surface ordering, both
in the field of molecular melts and of colloidal suspensions.

Contents

1. Introduction

The effect a surface or an interface may exert on the structure of an adjacent liquid phase has been a subject of scientific interest for almost two centuries. It dates back to the thesis of Poisson of 1831; he first claimed that there must be a deviation of order parameters close to a surface from their bulk values. A historical review of this subject is given by Ninham [1]. With the advent of surface sensitive scattering techniques, applying lasers and synchrotron radiation, it has become possible to study the structure of a fluid interface with molecular resolution. Far away from thermodynamic conditions at which the bulk fluid undergoes disorder $\rightarrow$ order phase transitions (subsequently called phase transition for simplicity), the structure of a liquid surface is mainly determined by a continuous density profile with an intrinsic thickness and thermally driven capillary waves. Experimental and theoretical contributions on this subject covering a large variety of systems from noble gases to metal melts were reviewed recently by Penfold [2].

If a liquid is in the vicinity of thermodynamic conditions (temperature, pressure and composition) at which a phase transition occurs in the bulk, in a layer close to an interface the transition may be shifted to different values of the thermodynamic variables of state by an adjoining substrate or gas phase. Thus a surface phase is in equilibrium with a bulk phase and a spectator phase. The latter may be a substrate or a vapour phase. On approaching the thermodynamic conditions for the bulk phase transition the thickness of the surface layer may diverge into the bulk. In this case the surface phase is said to completely wet the spectator phase. If the surface phase wets the spectator phase incompletely it will maintain a constant thickness of only a few molecular length scales upon approaching the bulk transition.

In the vast majority of cases the surface phase is less ordered than the bulk phase, as shown in figure 1. This situation is generally referred to as *surface melting*. It has been observed for a variety of metals [3–10] and molecular crystals. In particular, the surface melting of ice has been studied thoroughly [11–25].

The situation where a highly ordered surface phase is in equilibrium with a less ordered bulk and vapour or a spectator phase (i.e. an adjacent phase which does not influence the thermodynamic state of the sample) is called *surface freezing* or *surface ordering*. Although there is sound experimental evidence for atomic layering at the surface of metal melts [26], it appears that surface freezing occurs preferably with anisometric molecules, and consequently it was first observed with thermotropic liquid crystals. In one of the first systematic studies of the subject, Miyano measured the surface induced enhancement of the nematic order parameter of an isotropic liquid crystal melt [27, 28]. Later Als-Nielsen *et al* demonstrated that a smectic film is formed on top of a nematic bulk of a liquid crystal between the surface transition temperature, T_s, and the bulk transition temperature, T_b [29, 30]. In this case complete wetting of the vapour phase by the smectic film was observed. In the case of the isotropic/smectic A coexistence, Bahr and co-workers more recently found all types of known wetting behaviour, including first order wetting transitions [31, 32]. Thermotropic liquid crystals are widely used in displays, the operating mode of which is based on interface induced ordering [33]. This is probably the reason why most systematic studies of surface ordering in soft condensed matter systems have been conducted on thermotropic liquid crystals. This field of work is beyond the scope of this contribution, and deserves to be reviewed separately.

A classical example of surface freezing accompanied with incomplete wetting is the surface crystallization of long chain alkanes, which will be discussed in detail in section 3. There is an impressive amount of very accurate experimental data. Some computer simulations and thermodynamic theories are also available for these systems. However, a quantitative microscopic theory is still missing in this field. The opposite situation is encountered
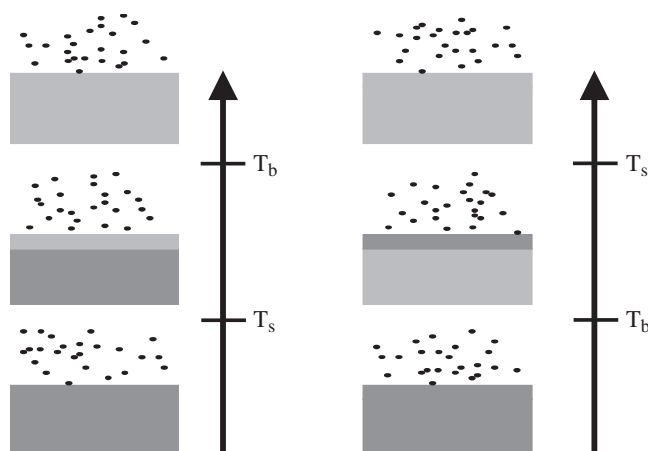
Figure 1. A schematic illustration of surface melting (left) where a less ordered (light grey) surface phase is in equilibrium with a more ordered (dark grey) bulk and the vapour phase at $T_s < T \leqslant T_b$; and surface ordering (right) where a more ordered surface phase is in equilibrium with a less ordered bulk and the vapour phase at $T_b < T \leqslant T_s$. The arrows indicate the direction of increasing temperature.

with colloidal solutions. There are very few systematic experimental studies on surface ordering effects, but there are microscopic theories available, which predict the surface phase behaviour qualitatively correctly. These theories require the knowledge of the particle pair potential and the interaction potential of a particle with the surface. For colloidal particles the latter can in principle be determined experimentally by techniques such as atomic force microscopy (AFM) [34], total internal reflection microscopy (TIRM) [35] or the surface forces apparatus (SFA) [36]. Since in colloidal systems these interaction potentials can be of very simple nature, it might well be that experimental data on surface freezing of colloid solutions could provide the basis for theoretical investigations of the subject, which in turn could have a stimulating effect on the development of theories for low molar mass systems. In the light of this assumption this topical review is organized as follows.

After a brief outline of surface sensitive scattering techniques in section 2, we will first focus on the surface ordering of simple chain molecules like long chain alkanes, alkenes and alcohols. Experimental findings, computer simulations and some theoretical approaches will be discussed in section 3. In section 4, mixtures and solutions of chain molecules will be treated. Finally we will review surface ordering effects in colloidal suspensions in section 5.

2. Scattering in reflection

2.1. General conventions

Any surface disorder $\rightarrow$ order transition will yield a surface layer with a density which is different from the bulk value. Consequently, the electron density and the scattering length density for neutrons of the surface layer will also be different from the bulk. Therefore surface sensitive scattering of x-rays or neutrons is the method of choice to study surface phase transitions which include a discontinuous change of an order parameter along the surface normal. In this section the principles of surface sensitive x-ray scattering will be briefly outlined with the understanding that the same formalism can be applied to neutrons as well.
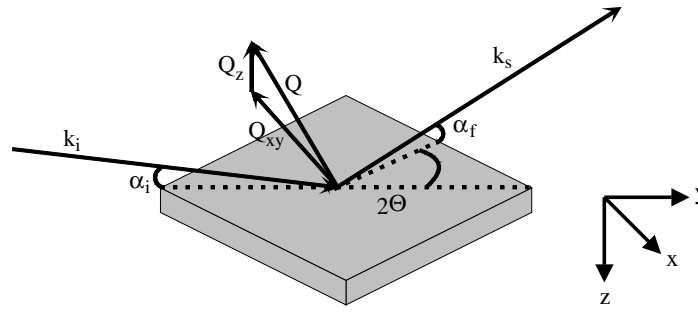
Figure 2. The definition of angles, real space directions and scattering vectors for a scattering experiment in reflection geometry.

The general scattering geometry for a scattering experiment in reflection is shown in figure 2. An incoming beam with wavevector $\mathbf{k}_i$ impinges on the surface, and the wavevector of the scattered beam $\mathbf{k}_s$ is determined by the position of the detection system which is fully defined by the in-plane angle 2θ and the reflection angle α_f. The scattering vector is defined as $\mathbf{Q} = \mathbf{k}_s - \mathbf{k}_i$, which usually for convenience is split into an in-plane part and a part perpendicular to the surface $\mathbf{Q} = \mathbf{Q}_{xy} + \mathbf{Q}_z$. The norm of either part is then given by $|\mathbf{Q}_{xy}| \equiv Q_{xy} = 4\pi \sin\theta/\lambda$ and $|\mathbf{Q}_z| \equiv Q_z = 2\pi(\sin\alpha_{ti} + \sin\alpha_{tf})/\lambda$, where λ is the radiation wavelength, α_{ti} is the angle which the transmitted incident beam spans with the surface, and α_{tf} is the angle between the surface and the scattered beam before it is refracted on leaving the sample. With this definition Q_z is the norm of the z-component in the material. In cases where refraction can be neglected, α_{ti} can be replaced by α_i and α_{tf} by α_f, respectively. Since the refractive index for condensed matter is smaller than unity [37], the incident beam will be totally reflected if $\alpha_i < \alpha_c$, the critical angle of total external reflection. In this region the sample is penetrated only by an evanescent wave which propagates in the direction of the projection of the incident beam onto the surface. For $\alpha_i \ll \alpha_c$ the minimum $1/e$-penetration depth is given by $\Lambda_0 = (16\pi r_0\rho_e)^{-1/2}$, where r_0 is the Thompson scattering length of a single electron and ρ_e is the electron density of the sample. As shown in figure 3, the penetration depth, Λ, increases when α_i approaches α_c, and jumps several orders of magnitude on passing α_c until Λ is only a function of the linear absorption coefficient of the sample at $\alpha_i \gg \alpha_c$. Thus it is possible to distinguish structural information either from a thin surface layer or from the sample bulk by simply varying the angle of incidence in a scattering experiment carried out in reflection geometry (XERD). Besides the XERD-experiment, where the full 3D scattering is probed, there are two basic types of experiments which can be performed during which certain geometrical restrictions are applied, i.e. diffraction at grazing incidence (GIXD) and specular reflectivity (XR), which will described in the following sections.

2.2. Grazing incidence diffraction

Grazing incidence diffraction (GIXD) was first developed to investigate the surface reconstruction of solid surfaces [38, 39]. It is a particularly powerful tool for the investigation of crystalline structures which are confined to a surface layer of well defined thickness, i.e. to two dimensions without a periodicity in the z-direction. In a scattering experiment on such a structure non-zero Bragg diffraction will occur if the incident wave propagates in the crystal plane and the h, k lattice lines are oriented such that they make an angle θ_{hk} with the propagation
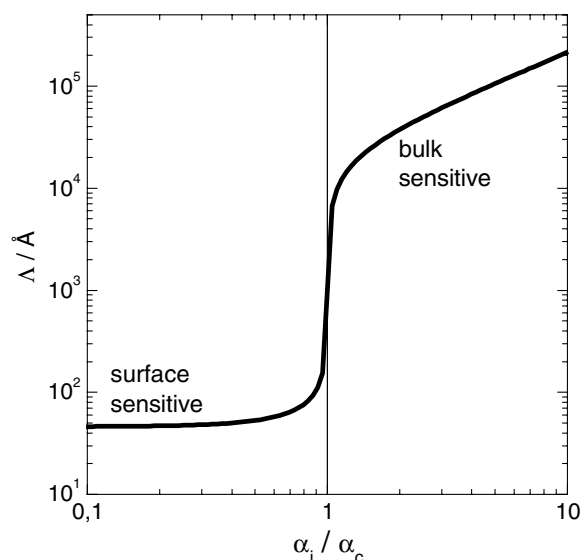
Figure 3. The penetration depth dependence on the angle of incidence of an x-ray beam with a wavelength of $\lambda = 1.54$ Å (Cu K$_\alpha$) impinging on a water surface. Due to the large variation of Λ a scattering experiment carried out at $\alpha_i \ll \alpha_c$ is sensitive to structures close to the interface, while at $\alpha_i \gg \alpha_c$ it is sensitive to bulk structures.

direction of the incident beam with $\lambda = 2d_{hk} \sin \theta_{hk}$, where h and k are the Miller indices of the two dimensional lattice and d_{hk} is the corresponding lattice distance which is related to the in-plane scattering vector by $d_{hk} = 2\pi/Q_{xy}$. Experimentally this can be realized in GIXD where $\alpha_i \ll \alpha_c$ and the resulting evanescent wave is diffracted by the lateral structure of the surface layer.

In the hypothetical case that the thickness of the 2D crystal in the z-direction is infinitely thin, all scattered waves which have the same Q_{xy} will have the same phase in the Fraunhofer limit. Therefore diffracted intensity will not be limited to discrete spots like in the case of 3D crystals, but will be evenly distributed along so-called Bragg rods, which are perpendicular to the surface and of infinite length. In real experiments, however, the Bragg rods will be of finite length due to the finite thickness of the crystalline layer.

For the examples to be discussed in this contribution, the two dimensional diffraction patterns can be analysed to a good level of accuracy with the routines which have been developed in the field of GIXD experiments from Langmiur monolayers [40, 41]. There the 2D crystals typically consist of a monomolecular layer of chain molecules with a length of some tens of Å and rotational symmetry. Thus the molecules are regarded as cylindrical bodies which are arranged in a two dimensional array with hexagonal or centred rectangular unit cells in which the cylinder long axes have a finite tilt angle with respect to the surface normal. For untilted cylinders the particle scattering factor is a disc lying parallel to the surface. In this case the superposition of the Bragg rods and the particle scattering factor leads to a maximum at $Q_z = 0$ of the intensity distribution along the z-direction of the rod. If the molecules are tilted their particle scattering factor is tilted accordingly, which leads to a maximum at $Q_z > 0$. Thorough analysis of the of the Bragg rods' intensity distribution along the z-direction eventually allows the determination of layer thickness, tilt direction and angle.
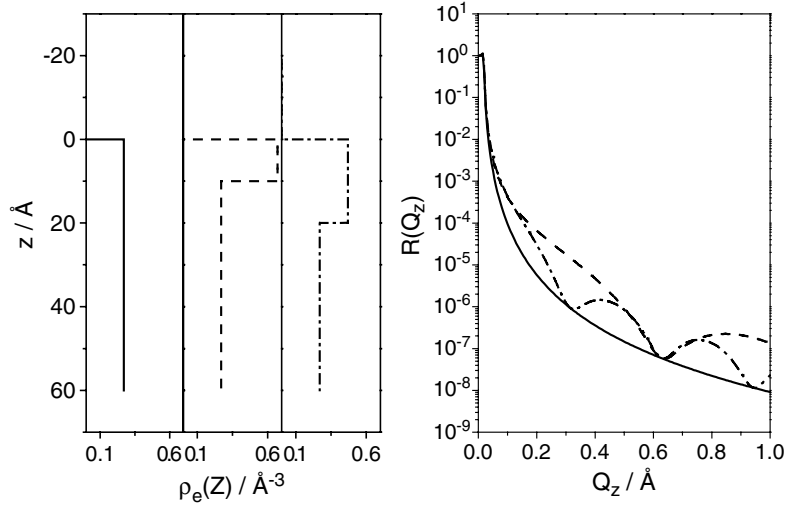
Figure 4. Left: model profiles of the electron density. Right: resulting reflectivity curves.

2.3. Specular reflectivity

In a specular reflectivity (XR) experiment the in-plane angle is kept at $2\theta = 0$ while the angle of incidence is varied typically from about zero to less than $3°$. Below α_c the beam will be totally reflected, while for $\alpha_i \geqslant \alpha_c$ it will be partially refracted into the sample volume and partially reflected. The intensity reflected under specular conditions ($\alpha_i = \alpha_f$), I_{spec}, is recorded independent of the angle of incidence, and normalized to the incident intensity, I_0, to yield the specular reflectivity as a function of Q_z, $I_{spec}/I_0 \equiv R(Q_z)$. Since in this particular geometry only scattering vectors normal to the surface are probed, $R(Q_z)$ is related to the Fourier transform of the electron density profile perpendicular to the surface $\rho_e(z)$.

$$R(Q_z) = R_F(Q_z) \left| \frac{1}{\rho_{e,\infty}} \int_{-\infty}^{\infty} \frac{d\langle\rho_e(z)\rangle}{dz} \exp\{iQ_z z\} \, dz \right|^2. \tag{1}$$

Here $\rho_{e,\infty}$ is the electron density of the bulk material and $R_F(Q_z)$ is the Fresnel reflectivity, as defined by equation (2), from a perfectly smooth surface of a sample with $\rho_{e,\infty}$. The angular brackets indicate that in an experiment, lateral variations of the electron density are integrated over the entire footprint area of the x-ray beam.

In the case of ordered surface layers this profile can be interpreted in terms of the thickness and lateral mean electron density of the film. The effect of various electron density profiles $\rho_e(z)$ on the specular reflectivity is displayed in figure 4. For a simple step-like profile, where the electron density jumps from zero to the bulk value $\rho_{e,\infty}$, the reflectivity decays monotonically following Fresnel's law:

$$R_F(Q_z) = \left| \frac{Q_z - \sqrt{Q_z^2 - Q_c^2}}{Q_z + \sqrt{Q_z^2 - Q_c^2}} \right|^2 \tag{2}$$

where Q_c is the scattering vector corresponding to α_c. A layer with enhanced electron density of thickness d on top of the sample will cause undulations in the reflectivity curve. While the amplitude of these undulations is related to the difference $\rho_e - \rho_{e,\infty}$, the distance between

two adjacent minima is roughly given by $\Delta Q_z \approx 2\pi/d$. A parameterized description of the electron density profile can be obtained by nonlinear least squares fitting of a so-called box- or slab-model. The formalism outlined above is usually referred to as the kinematic approximation. Although it neglects refraction and multiple scattering, it is accurate enough for most applications, if refraction is introduced *a posteriori* by using $Q_z = 4\pi \sin\alpha_t/\lambda$, where α_t is the angle of the refracted beam with the surface. For an exact formalism, the reader is referred to the pioneering paper of Parratt [42], and for an overview of model independent approaches to data analysis see [43].

3. Surface ordering of pure liquids

3.1. Alkanes

Surface freezing of long chain alkanes was reported to manifest even in macroscopic observables. Shaking of melts of pure alkanes and derivative materials leads to foam formation in a well defined temperature range above the melting temperature. This surprising phenomenon was reported as early as 1954 [44]. In the same temperature range macroscopic particles spread on the melt surface were seen to move with remarkable lateral speed (Marangoni flow). Performing quantitative measurements of the foam stability and the lateral speed as a function of temperature, Gang *et al* [45] showed that both effects are related to the formation of a monomolecular quasi-crystalline layer at the liquid–vapour interface.

The first systematic study of surface freezing had been reported six years earlier by Earnshaw *et al* for melts of alkanes with carbon numbers $15 \leqslant n \leqslant 18$ [46]. They observed a positive temperature gradient of the surface tension, $\mathrm{d}\gamma/\mathrm{d}T$, directly above the bulk melting temperature of the alkane, T_b, which became negative about three kelvin above T_b. Since $\mathrm{d}\gamma/\mathrm{d}T$ is the negative surface excess entropy, this finding was interpreted as surface induced pre-freezing which occurs at the temperature of the sign change, T_s. Further, the authors argued that the surface freezing was limited to a few molecular length scales at most. The latter point was confirmed shortly after by Ocko *et al*, on the basis of XR experiments [47, 48]. Above T_s, the reflectivity curves show a monotonic decay, while they exhibit undulations in the temperature range $\Delta T = T_s - T_b$, as is shown in figure 5. The deduced electron density profiles show that there is a condensed layer on top of the sample with an electron density roughly 20% higher than the bulk value. The layer thickness corresponds nicely to the length of the hydrocarbon chains, indicating a monomolecular layer. In figure 6, the reflected intensity at fixed Q_z and the surface tension are plotted versus temperature. The surface freezing is clearly visible from the sudden increase of intensity at T_s and the change of sign of the surface tension temperature gradient. Throughout the entire range of ΔT the reflectivity and $\mathrm{d}\gamma/\mathrm{d}T$ remains constant, indicating that no further structural changes occur.

Using GIXD the authors could further show that the surface layer was quasi-crystalline with a positional correlation length in the micrometre range [47]. The complete series of hydrocarbons with carbon numbers covering a range of $14 \leqslant n \leqslant 50$ was subsequently studied by the same group [49, 50]. Although there is some controversy as to whether the smallest carbon number at which surface freezing occurs is $n = 15$ [49] or $n = 16$ [50], it is evident for the whole series that the surface frozen region is limited to a monomolecular layer for all carbon numbers investigated. That is, the ordered phase does not wet the surface completely, contrary to what was observed for many liquid crystalline systems.

The lateral structure of the monolayers depends on the carbon chain length. For $n < 30$ it was reported to be a rotator phase of hexagonal symmetry with the molecules aligned parallel to the surface normal. In the range of $30 \leqslant n < 44$ the structure is still a rotator phase with
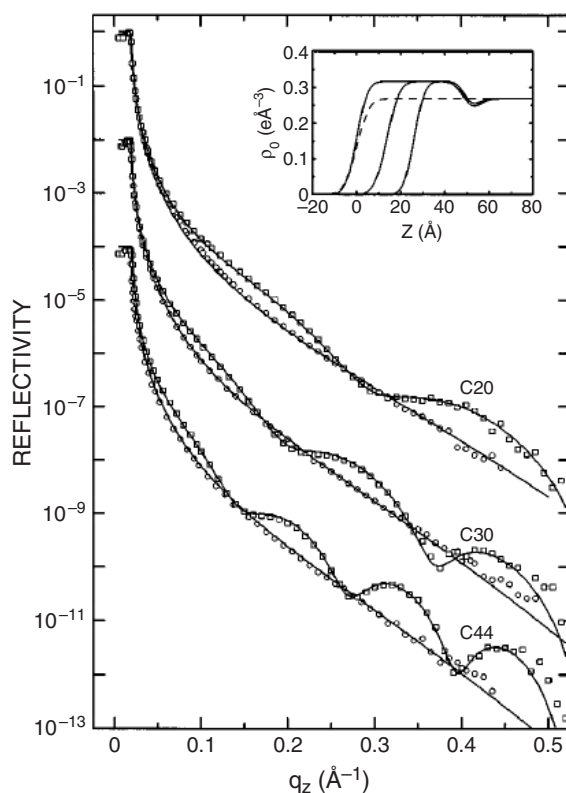
Figure 5. Reflectivity curves of alkane surfaces with $n = 20$, 30 and 44 above T_s (○) and at $T_b < T \leqslant T_s$ (□). The full lines are fits with a two-box model. The corresponding electron density profiles shown in the inset are dashed above T_s and solid for $T_b < T \leqslant T_s$. (Reproduced with permission from [50] © by the American Physical Society.)

centred rectangular symmetry, and the molecules are tilted towards their nearest neighbour. The tilt angle increases continuously with the chain length. Finally, above $n = 44$ the structure is crystalline with a next-nearest neighbour tilt.

The temperature range, ΔT, in which the surface layer exists increases steeply from zero at $n = 15$ to roughly 3 K at $n \approx 20$, then decreases almost linearly to $\Delta T \approx 2.5$ K at $n = 44$ and finally drops off sharply to $\Delta T \approx 0.5$ K at $n = 50$. A semi-empirical model was derived which describes very well the dependence of ΔT on the carbon number for $n \leqslant 44$. The model is based on the variation of entropy and excess free energy in the surface layer with chain length, where the interaction energy is assumed to be of van der Waals type. The breakdown of this model is ascribed to the switch from a rotator-like to a crystalline 2D structure of the layer at $n = 44$.

On the other hand, Pfohl *et al* came up with an alternative model for the surface frozen layer for heptadecane and eicosan [51]. They observed a change in the ellipsometric signal at T_s, which was however so small that the authors found it difficult to explain within the model discussed above. Therefore they suggested that the alkane chains in the region near the surface are preferentially oriented normal to the surface in a nematic-like structure well above the surface freezing temperature. At T_s a transition occurs from the nematic-like to a smectic-like monolayer with almost the same density as the nematic state. No penetration of the bulk phase
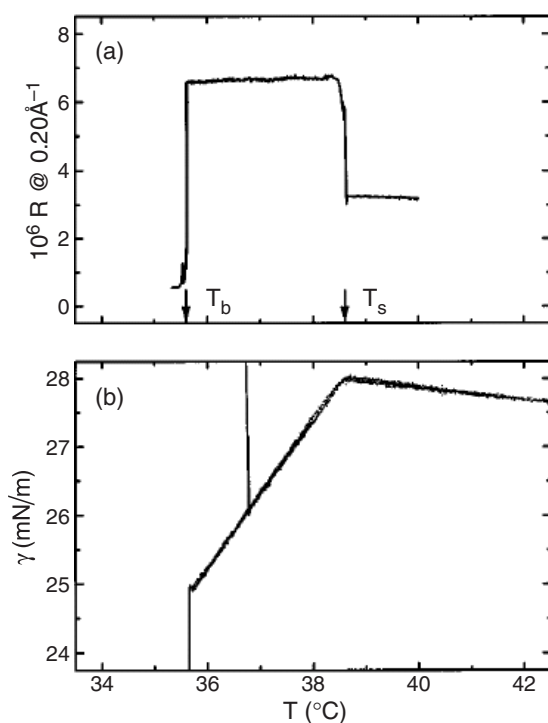
Figure 6. The temperature dependence of the reflectivity at fixed Q_z (a) and the surface tension (b) of an *n*-eicosane surface. The transition, from a liquid surface to a surface frozen layer at T_s, is manifest from the sharp intensity jump in (a) and the abrupt change of slope in (b). (Reproduced with permission from [50] © by the American Physical Society. Note that the transition temperature labels are exchanged in the original paper.)

into the monolayer is allowed which generates a density gap between the smectic surface layer and the underlying bulk. This gap causes x-ray interferences which can well describe the x-ray reflectivity experiments by Wu *et al* despite the equality of bulk- and surface density, which in turn allows for the observed small change of the ellipsometric signal at T_s.

Further studies applying surface forces measurements [52, 53] and differential thermal analysis and ultraviolet photoemission [54] also detected a surface phase transition accompanied by the stabilization of a more ordered phase towards higher temperature at the surface. However, these techniques do not provide any information on the structure of the surface, and thus these results cannot help to distinguish the alternative structural models.

The situation is further complicated by the fact that the structure of the frozen surface layer appears to depend also on the nature of the spectator phase. Experiments on the interface between SiO$_2$ covered silicon wafers and alkane melts suggested the formation of an interfacial layer in which the molecules are oriented perpendicular to the interface below T_s [55–57]. However, these findings were contradicted by Volkmann *et al* [58] in the sense that in the first layer on top of the SiO$_2$ the molecules are oriented parallel to the interface, followed by a layer with perpendicular orientation. Parallel orientation of the first alkane layers is similar to what was reported earlier on normal alkanes adsorbed to solid substrates [59–62].

Using sum frequency generation spectroscopy, Yeganeh [63] studied the phase transition and molecular arrangement of alkanes at an Al$_2$O$_3$ interface. It was observed that this particular interface does not change the transition temperatures from their bulk values. In the solid state

the chain molecules lie on the substrate with the C–C axis parallel to the interface and the molecular plane perpendicular to the substrate normal.

The phenomenon of surface freezing has been tackled theoretically and by applying computer simulations by several groups. Leermakers *et al* [64] modelled the orientational ordering aspect of the surface freezing of *n*-hexadecane with a self-consistent field lattice gas theory, showing that it is a first order transition. Ocko *et al* propose a simple model which explains surface freezing purely on the basis of the interfacial tensions of the two participating interfaces [50, 65], i.e. between the melt and the surface layer and between the surface layer and the vapour phase. On the other hand, Tkachenko *et al* [66–68] propose that additional entropy contributions due to fluctuations of the alkane chains in the directions of their long axis have to be taken into account for the calculation of the free energy of the system.

Various simulation studies reproduced the experimental findings in part, but failed to in important details. All simulation studies find the formation of a frozen surface layer with perpendicular orientation of the chain molecules; however, as opposed to the x-ray experiments, Li *et al* find surface freezing for chains as short as $n = 11$ [69, 70]. The simulation studies of Shimizu *et al* [71] reveal that the surface layer is in thermal equilibrium with the melt through frequent molecular exchanges. Further it is shown that the molecules have high lateral mobility and a broad positional distribution of centres of mass along the surface normal. In this sense these simulations are in favour of the fluctuation scenario by Tkachenko *et al*. However, it was also found in this investigation, that slow stepwise cooling will lead to multi-layer formation, which is not observed in experiments. On the other hand, early simulations by Xia *et al* also showed enhanced positional correlation for four molecular layers on top of melts of hexadecane and heptadecane [72]. Probably the best agreement so far with experiments was found in simulations of heptadecane by Smith *et al*. These authors also find that the properties of the surface chains are in accord with the model of a fluctuation stabilized layer [73]. The layer was found to be ordered, yet not crystalline, and the molecules are able to diffuse in the plane of the surface and perpendicular to it. However, it is not clear whether the degree of order would allow for the resolution limited GID peaks which have been observed experimentally [50].

3.2. Alkenes, alcohols and semi-fluorinated alkanes

In this section, surface freezing of chain molecules, which are different from alkanes in either of two respects, will be discussed. Alkanes interact mainly via van der Waals potentials, and these interactions are invariant to the inversion of the molecules about their centres of mass. We will see in the following that breaking either of these conditions will grossly alter the structure and phase behaviour of surface frozen layers.

The simplest case, where the symmetry of the chain is broken by the introduction of a C–C double bond, was studied by Gang *et al* for the case of α-eicosene [74]. They found that the structure of the surface frozen layer was very similar to that of the corresponding normal alkane. However, the temperature range in which the surface layer is stable is larger for the α-eicosene as compared to the saturated chain. This is ascribed to the entropy gain associated with flipping of the molecules, which is apparently not over-compensated by the corresponding energy cost.

A much greater variety of structures and phase behaviour was observed for normal alcohols, i.e. hydrocarbon chains carrying an OH substituent at one of the terminal carbon atoms [75–77]. Surface freezing of alcohols was discovered first by Deutsch *et al* [75]. Also in the case of alcohols with even carbon numbers, a 2D crystalline layer is formed which maintains constant thickness throughout the entire temperature range, ΔT, in which it is stable. For chain lengths of $n \leqslant 22$, the lateral structure of the layer is hexagonal with the

chains oriented perpendicular to the surface, while it is centred rectangular with a next-nearest neighbour tilt for longer chains.

With $\Delta T \lesssim 1$ K it is somewhat smaller than observed for alkanes. However, the major difference from the behaviour of alkanes concerns the structure along the surface normal. The surface frozen layer of an alcohol melt consists of two molecular sheets, i.e. it is a *bi*layer. The x-ray reflectivity data show an enhanced electron density in the centre of the layer corresponding to head-to-head stacking of the OH groups. Analysis of the GID data suggest that the bottom layer is displaced laterally with respect to the top layer, such that the OH groups of the bottom layer are located below the voids of the hexagonal unit cells of the top layer. This arrangement of the OH groups allows for the stabilization of the bilayer by hydrogen bonding. A second remarkable deviation from the alkane behaviour is the fact that surface freezing occurs only with alcohols of even carbon numbers in the range $16 \leqslant n \leqslant 28$. This odd–even effect was ascribed to differences in the orientation of the terminal OH group relative to the molecular axis, which may render the formation of hydrogen bonds unfavourable in odd alcohols by making the relevant HO–H distances deviate from the required value of $\sim$2.8 Å [78].

As the capacity for hydrogen bond formation causes qualitative differences between the structure of surface frozen alkanes and alcohols, it is to be expected that additives which are able to form hydrogen bonds as well will further alter the surface structure of alcohol melts. Investigations of alcohols in equilibrium with a water saturated atmosphere [76, 77] show on one hand that the basic features of the bilayer structure are not changed except for a swelling of the bilayer due to intercalation of water into the OH group region. Normal to the surface, the bilayers grow by $\sim$3% independently of the alcohol chain length. Parallel to the surface, an expansion of the unit cell dimensions by $\sim$2% was observed only for the non-tilted systems. On the other hand, an enormous increase of ΔT due to hydration was observed, together with an expansion of the range of chain lengths in which surface freezing occurs. Differently from the dry alcohols, surface freezing occurs down to chain lengths of $n = 12$ in hydrated systems, and the temperature range is expanded roughly by a factor of two. These effects were accounted for quantitatively, by considering the hydration levels of the bulk and the surface, and taking into account the differences in that level due to adsorption or depletion of water at the surface. For a detailed description of this consideration, the reader is referred to the paper by Gang *et al* [77]. The variability of phase behaviour and structure of frozen surface layers may be further enhanced by suitable additives, which will be discussed in section 4.

A further class of chain molecules which show surface freezing are semi-fluorinated alkanes (SFA), i.e. carbon chains which are carrying hydrogen and fluorine atoms in a block-wise arrangement: $F_m H_n$, where m denotes the number of fluorinated carbon atoms and n is the chain length of the hydrocarbon block. Like alkanes, these molecules have only van der Waals interactions, but the symmetry of the interaction potential upon flipping the chains is severely perturbed. Miscibility studies of hydrocarbon and fluorocarbon solvents have shown [79] that the free energy of transfer of a CH_2 group into fluorocarbon and a $-CF_2$ group into hydrocarbon are approximately 1.1 and 1.4 kJ mol^{-1}, respectively. These values imply that the antipathy between hydrocarbon and fluorocarbon chains is about 1/3 of the free energy of transfer of $-CH_2$ groups from alkane to water. Further, the structure within the two blocks is different: a planar zig-zag chain in the $-CH_2$ block with a cross sectional area of $\sim$18 Å, and a rigid helix in the $-CF_2$ block with a lateral spatial requirement of $\sim$28 Å. A series of $F_{12}H_n$ (with $n = 8$, 14 and 19) melts was investigated with regard to surface freezing by Gang *et al* [80]. In the cases of $n = 8$ and 14, the authors found surface frozen layers with a thickness which corresponds to the length of a completely stretched molecule, indicating a surface normal orientation. The electron density profiles deduced from XR data by fitting to a two slab model clearly show that the F blocks point to the vapour phase. However, a

detailed analysis of the profiles reveals that the two slabs cannot be simply identified with a close packing of the fluorinated and the hydrogenated block. Neither of the widths of the slabs coincide with the nominal lengths of the two blocks, nor do the electron densities with those of closely packed F blocks and H blocks, respectively. These discrepancies were accounted for in a model of an up–down staggering of the molecules, which is probably brought about by the helical screw-like structure of the F block. This would lead to lateral modulations of the surface frozen layer similar to that observed in the undulating lamellar phases of bulk $F_{12}H_n$ [81]. The behaviour of the long chained $F_{12}H_{19}$ was found to be even more complex. Contrary to all systems described so far, the thickness and the density of the surface frozen layer vary in a complex manner with temperature. Surface tension measurements as well as XR experiments indicate a continuous transition from the surface frozen to the liquid state. Further, no GIXD spectra could be observed at any temperature, indicating a disordered state of the surface layer. The authors suggest a buckled structure for this surface layer driven by the different cross sectional areas of the respective blocks, and leading to a dome-covered surface with large voids. This model accounts for the temperature dependence of the layer thickness and the disordered structure as well as for the surprisingly low electron density which was observed.

4. Liquid mixtures

As we have seen in section 3, the structure and the phase behaviour of surface frozen layers of chain molecules is dominated by a subtle energy–entropy balance. Consequently, one may expect novel effects in mixtures of chain molecules, since mixing introduces a further source of entropy.

Studies of mixtures of alkanes (denoted C_n and $C_{n+\Delta n}$) with different chain lengths n and $n + \Delta n$ by Wu et al [82, 83] show that the chain length mismatch, Δn, has a drastic impact on the structure of the surface frozen layer. For small Δn, the properties of the surface layer change continuously from those of a pure $C_{n+\Delta n}$ layer to those of a pure C_n layer with the bulk volume fraction of the short chain component, ϕ_{C_n}. No further structural changes were observed either by varying temperature or as a function of bulk composition.

By contrast, mixtures with large Δn show a discontinuous transition from a pure $C_{n+\Delta n}$ layer to pure C_n layer as the bulk composition is varied, and an additional new transition involving a change of tilt angle and direction which occurs as a function of bulk composition. As indicated in figure 7, this transition can also be induced by temperature changes, which is a novelty for surface frozen layers of alkanes. The observed phenomena could be well accounted for in the framework of a Flory–Huggins type theory which is based on the balance of mixing entropy and repulsive energy due to the chain length mismatch.

A different scenario was observed for mixtures in which the short chain component does not show surface freezing in its pure state [84]. Here the surface frozen layer maintains the same structure as in the pure $C_{n+\Delta n}$ case until it ceases to exist, if ϕ_{C_n} exceeds a certain value.

Mixtures of alcohols with different chain lengths show a qualitative similar Δn dependence as alkanes [85, 86]. However, there is a remarkable difference in that long chain alcohols induce surface freezing of alcohols which do not show surface freezing if they are pure. The addition of 10% $C_{18}OH$ to $C_{12}OH$ induces the formation of a $C_{12}OH$ frozen bilayer in the appropriate temperature range [85]. In mixtures of $C_{14}OH$ and $C_{18}OH$ the properties of the surface frozen layer changes continuously from a pure $C_{14}OH$ bilayer to a pure $C_{18}OH$ bilayer with increasing bulk fraction of $C_{18}OH$ [86]. Note that neither pure $C_{12}OH$ nor pure $C_{14}OH$ show surface freezing, which indicates that the surface phase behaviour of alcohol melts can be tuned by appropriate additives.
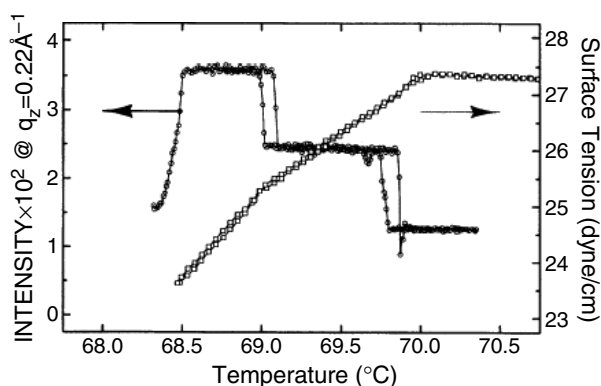
Figure 7. The temperature dependence of the reflectivity at a fixed Q_z (left-hand axis) and of the surface tension (right-hand axis) from a C_{26}–C_{36} mixture at $\phi_{C_{26}} = 0.41$. The formation of the surface frozen layer at $T_s \approx 70\,^\circ\text{C}$ and the transition to a new phase at $T_n \approx 69\,^\circ\text{C}$ are seen as jumps in the reflected intensity and as slope changes in the surface tension. (Reproduced with permission from [82] © by the American Physical Society.)
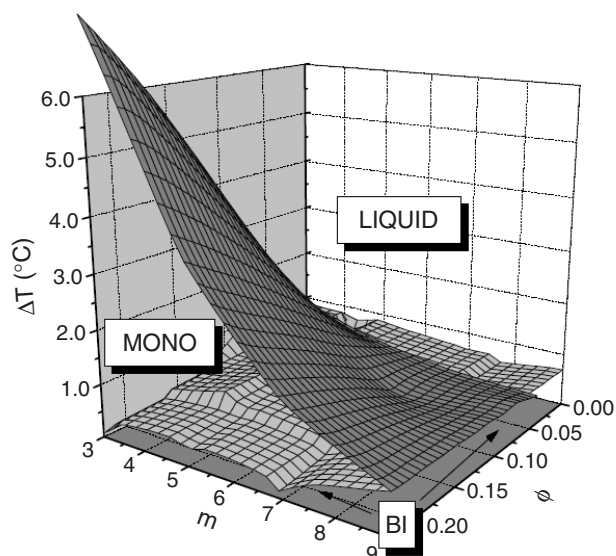

Figure 8. Surface phase diagram of α, ω-diol:C_{20}OH melts. ΔT is the temperature difference from the bulk freezing temperature T_f, ϕ is the molar fraction and m is the chain length of the diol. (Reproduced with permission from [89].)

This effect was extensively studied by the addition of short chain α, ω-diols, i.e. hydrocarbon chains carrying an OH group on both terminal carbons, to long chain alcohols [87–89]. It was observed that the surface frozen layers of alcohols can be effectively tuned from bilayer to monolayer structure by addition of α, ω-diols with different chain lengths m. The resulting (T, ϕ, m) phase diagram is displayed in figure 8. At molar fractions greater than 0.06 of α, ω-diol in C_{20}OH melts, a monolayer phase appears when the samples are heated from the surface frozen state to the liquid state. The temperature range in which this monolayer exists becomes broader with increasing bulk concentration of the diol, while it shrinks with

increasing carbon number m of the diol. The observed phase diagram could be well predicted by a simple theory, which assumes a linearized dependence of the free energies of the various interfaces in each phase on the diol content.

The subtlety of the energy–entropy balance which determines the surface structure of alcohol melts is emphasized by the observation of a quadrilayer structure which was reported very recently [90]. Mixtures of $C_{18}OH$ and $C_{26}OH$ have a narrow range of compositions, $0.2 \lesssim \phi_{C_{26}} \lesssim 0.23$, in which cooling of the melt leads to the usual surface frozen bilayer which is followed by a quadrilayer structure before bulk freezing. It is not clear so far whether this is a hint of a chain length or composition driven wetting transition from partial to complete wetting.

A thermodynamic theory which accounts well for the surface phase behaviour of a wide variety of alkane mixtures as well as alcohol mixtures was given in two very recent papers [91, 92]. The theory is based on a regular mixture approach for the bulk, which takes into account the entropy of mixing and a phenomenological energy contribution, ω, due to the interchange of two alkane molecules with different chain lengths in the crystalline phase. To describe the surface phase behaviour the composition of the surface (which is different from the bulk mixture) was calculated on the basis of the Gibbs adsorption rule. Balancing the chemical potentials of either component in either surface phase (equilibrium condition) yields expressions for the dependence of T_s and the surface excess entropy, ΔS^s, on the mixture composition with ω as the only adjustable parameter. Fitting of these expressions to the experimental data shows that ω depends linearly on $(\Delta n/\bar{n})^2$, where $\bar{n}$ is the mean chain length of the mixture. This behaviour was found to be universal for all alkane mixtures, dry alcohol mixtures and even for hydrated alcohol mixtures, if the contribution of the water to the mixing entropy is taken into account to first order.

For the sake of completeness we mention here that solutions of semi-fluorinated alkanes in hydrocarbons have also been investigated concerning their surface phase behaviour [93–96]. However, in these studies the formation of an ordered SFA surface layer was observed at very low concentrations. It is therefore very likely that the layer formation is adsorption driven, and not a surface freezing effect.

5. Colloidal suspensions

Compared to the enormous number of studies of surface freezing effects in molecular liquids, there are only very few contributions on surface induced ordering of colloidal suspensions under comparable conditions. There are investigations on two dimensional colloidal systems, e.g. [97, 98], and on surface induced ordering by patterned substrates, e.g. [99, 100]. The present discussion will, however, be restricted to three dimensional dispersions which show surface ordering induced by an energetically homogeneous spectator phase.

Solutions of surfactants or amphiphilic blockcopolymers are particularly interesting for the investigation of surface effects, since they show a wealth of phases [101–105] with various micro-structures on relevant length scales in the colloidal domain. Binary water + surfactant mixtures form isotropic micellar solutions at low surfactant contents and lyotropic liquid crystalline phases of different symmetry at high volume fractions of the surfactant. In ternary water + surfactant + oil mixtures so-called microemulsions can be obtained. Depending on the system composition, microemulsions either consist of oil droplets dispersed in water, or a bicontinuous sponge-like structure or water droplets dispersed in the continuous oil phase. The effect of a macroscopic surface on the structure of a droplet microemulsion was first investigated by Schwartz *et al* [106]. In the system water + AOT (sodium di-2-ethylhexylsulfosuccinate) + decane these authors could not detect any difference of the droplet size and distance at
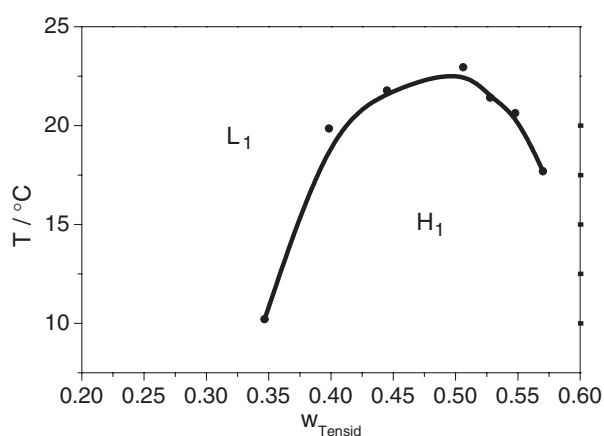
Figure 9. The coexistence line in the temperature–composition plane of the isotropic L_1 phase with the hexagonal H_1 phase in the bulk of aqueous $C_{12}E_5$ solutions. Compositions are given as surfactant weight fractions w_{Tensid}. The data points were read off graphically from [108] and the full curve is just a guide to the eye.

the surface as compared to the respective bulk values. An entirely different behaviour was observed at the surface of a bicontinuous microemulsion of the system $D_2O + C_{10}E_4$ (tetra-(ethyleneoxide)-n-decylether) + decane. Chou *et al* [107] showed, by neutron reflectivity experiments, that the surface induces a lamellar stacking of alternating water and oil layers which relaxes to the bicontinuous bulk structure along the surface normal.

Surfactants of the oligo-(ethyleneoxide)-n-alkylether type with the general chemical composition $CH_3(CH_2)_{m-1}(OC_2H_4)_nOH$ (abbreviated as C_mE_n) consist of a hydrocarbon tail which is hydrophobic and a water soluble oligo-(ethyleneoxide) headgroup. If dissolved in water, they form micelles at concentrations above a so-called critical micellization concentration (cmc). Depending on the relative volumes of the molecular moieties, the shape of these micelles can be either spherical, ellipsoidal or thread-like. Upon increasing the concentration, solutions containing thread-like micelles will transform into a lyotropic liquid crystalline phase, denoted H_1, in which the micelles are arranged on a two dimensional hexagonal array with their long axis aligned in parallel. The coexistence line of the isotropic micellar phase, L_1, and the H_1 phase of the $C_{12}E_5$ + water is sketched in figure 9 [108].

The effect of the macroscopic solution vapour interface on this coexistence line was investigated by Braun *et al* [109–112]. The authors showed that the free surface has an impact on the phase behaviour and the structure near the surface in a threefold way.

First, the hexagonal arrays are forced to align such that the orientation of the (01) lattice plane is parallel to the surface with a variation of less than 3°. This is demonstrated by the diffraction pattern shown in figure 10, which was recorded in reflection geometry. The occurrence of Bragg diffraction peaks shows that there are only discrete orientations of lattice planes with respect to the surface plane. The surface alignment persists several micrometres away from the surface into the bulk, as was shown by x-ray reflectivity experiments [111]. On the other hand, the cylinder long axes were shown to be oriented randomly in the surface plane. That is, the H_1 phase has to be regarded as a powder sample in the surface plane and as being monocrystalline in the direction along the surface normal.

Second, closer inspection of figure 10 reveals that the diffraction pattern consists of a set of hexagonally arranged doublet peaks, which is strong evidence for the existence of two
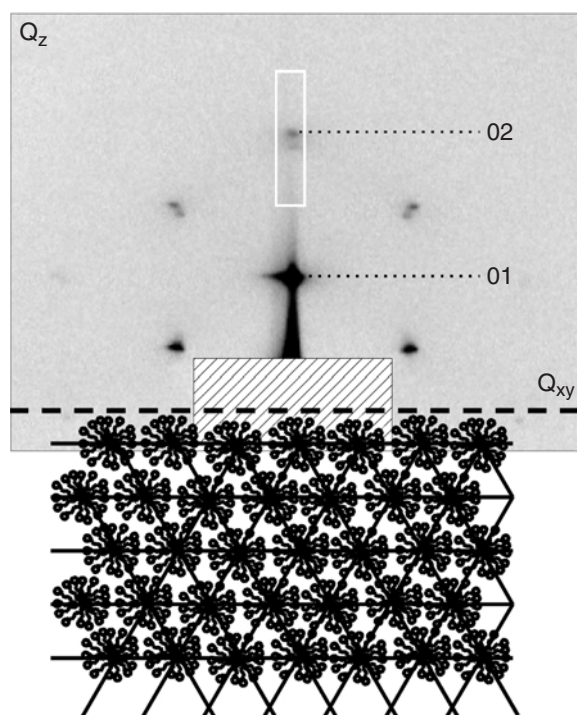
Figure 10. Top part: a two dimensional diffraction pattern recorded in reflection geometry from a $C_{12}E_5$ + water mixture with a surfactant content of 50% by weight at 22 °C. Note the doublet character of all diffraction peaks. The numbers are the Miller indices of the peaks which have only a Q_z contribution to the scattering vector. The white rectangle indicates the location of the linear position sensitive detector which was used to record the spectra displayed in figures 11 and 12. The shaded area marks the position of a primary beam stop. Bottom part: a sketch of the real space geometry in the H_1 phase. The cylindrical micelles are arranged on a two dimensional hexagonal array with their long axes normal to the paper plane.

hexagonal lattices with different lattice constants in real space. In figure 11, the intensity of the (02) peak at various angles of incidence is plotted versus Q_z. On increasing the angle of incidence, i.e. going from surface sensitive to bulk sensitive scattering geometry, one of the two peaks vanishes. Systematic fitting of the data with a model function shows that the area ratio of the two peaks $r = A_{\mathrm{high}Q_z}/A_{\mathrm{low}Q_z}$ decreases gradually from $r \approx 2.5$ at small angles of incidence to $r \approx 0.75$ at the highest α_i. This shows that the lattice which causes the scattering peak at high Q_z is present only in a near surface region. Consequently, there has to be a layer close to the surface where the lattice constant is reduced as compared to the bulk, i.e. the surfactant volume fraction in this layer is higher than in the bulk. It is not immediately evident why both the surface and the bulk peak can be observed at angles of incidence smaller than the critical angle of total reflection α_c. This is due to the fact that the surface becomes macroscopically rough, i.e. cluttered with grains, which are visible to the naked eye, when the sample enters the hexagonal phase. Consequently, the angle of incidence may locally be very different from the experimentally preset value. Therefore, refraction of the incident and the scattered beam on entering and respectively leaving the sample cannot be taken into account properly in the data analysis, and the authors neglected refraction completely. An appropriate correction to Q_z for smooth surfaces at low angles would be $Q_z^{\mathrm{corr}} = Q_z + Q_c/2$, where the
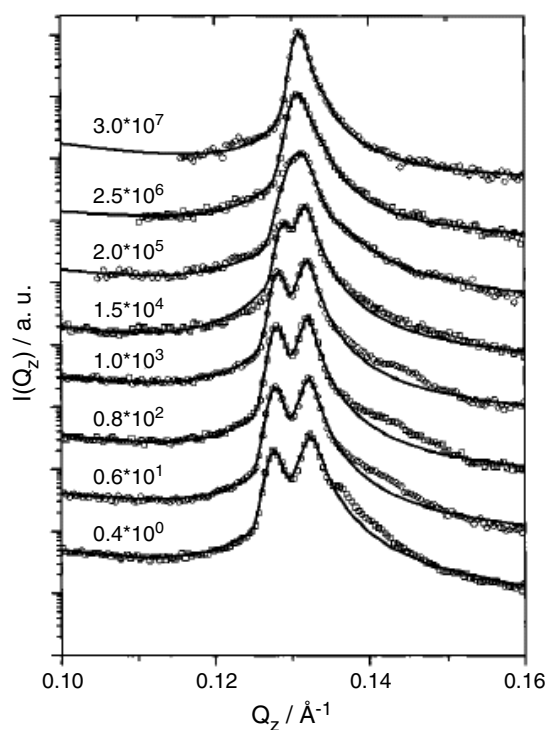
Figure 11. The intensity distribution of the (02) peak along the surface normal from a $C_{12}E_5$+water mixture with a surfactant content of 50% by weight. A linear position sensitive detector was located at the position indicated by the white rectangle in figure 10. The numbers above the curves indicate the multifolds of α_c at which the data were recorded multiplied by the factors used to shift the curves on the ordinate. The temperature was kept constant to ± 0.01 K. (Reproduced with permission from [110] © by the American Chemical Society.)

second term is half the critical wavevector. For the curves recorded at $\alpha_i < \alpha_c$ this would lead to an systematic error of the scattering vectors of approximately 8–10%, which gave rise to speculations that the peak at higher Q_z might be merely an artefact due to refraction. However, for $C_{12}E_5$+water mixtures $Q_c \approx 0.022$ Å^{-1}. Thus the $Q_c/2$ correction to the scattering vector is about 1.5–2 times larger than the separation between the two peaks. Refraction alone can therefore not explain the occurrence of the higher Q_z peak. On the other hand, the amount of the correction matches the scattering vector difference between the surface peak and the additional scattering in the range 0.135 Å $< Q_z <$ 0.145 Å, which occurs at low angles of incidence. Since the authors give no other explanation for these halos in the original paper it is tempting to speculate that they are caused by refraction. For grains with a surface which locally make an angle smaller than α_c, the $Q_c/2$-correction would apply, and the surface lattice peak would be shifted by approximately 0.011 Å. The intensity of these peaks would depend on the fraction of grains which have the adequate orientation. Since the evanescent wave probes only a few periods of the underlying lattice, the peaks would be correspondingly broad, and they would sharpen with increasing α_i.

The authors argue that the coexistence of two isostructural phases with different densities is due to the lateral pressure which the micelles at the interface experience. A similar effect though in bulk dispersions has been reported by Bolhuis *et al* [113]. On the basis of Monte Carlo simulations it was predicted that sterically stabilized colloids will undergo pressure driven
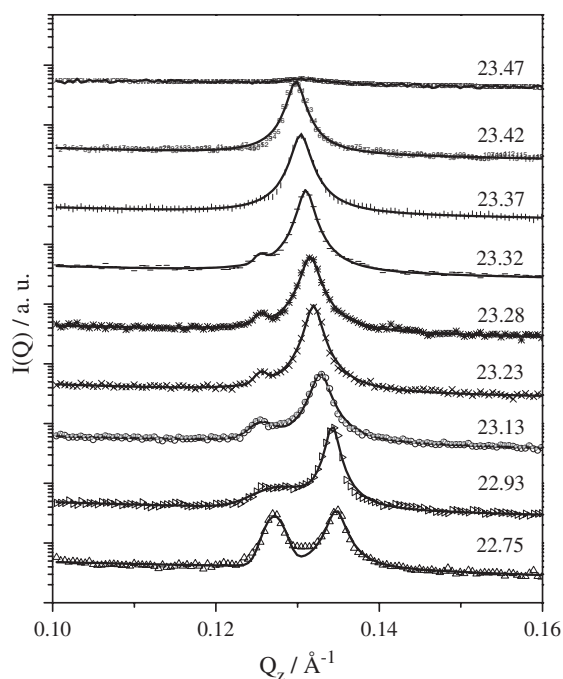
Figure 12. The intensity distribution of the (02) peak along the surface normal from a $C_{12}E_5$+water mixture with a surfactant content of 50% by weight. The spectra were recorded at constant angle of incidence. The numbers indicate the sample temperature in °C.

isostructural phase transitions, if their pair interaction potential has a secondary potential minimum due to short range attractions. Accordingly, shrinking of the lattice constant as observed by Lang *et al* [110] might be induced by the pressure tensor asymmetry at the surface.

Third, it was demonstrated that the system exhibits surface freezing. This is evident from figure 12, where the intensity distributions of the (02) peak along the surface normal are displayed as a function of temperature. There is clearly a temperature range in which the diffraction peak at low Q_z has vanished while the high-Q_z peak is still prominent. This shows that the bulk solution is in the isotropic state while the surface region is in the hexagonal state at the same temperature.

From the second and third points it follows immediately that the L_1–H_1 coexistence line is shifted to higher surfactant concentrations and to higher temperatures as compared to the bulk phase behaviour. To our knowledge this was the first investigation to conclusively show a surface induced shift of a phase transition in colloidal dispersions.

As opposed to molecular melts, surface ordering in colloidal suspensions was observed also with spherical particles. This effect was first predicted on the basis of molecular dynamic simulations [114, 115], and experimentally reported by Gestenberg *et al*. These authors have investigated solutions of spherical blockcopolymer micelles [116–118] which can be modelled as a system with hard body interactions. Deep in the isotropic region of the bulk phase diagram the authors observed a broad peak in the neutron reflectivity curve. Thorough data analysis revealed an undulating scattering length density profile along the surface normal which decays to the bulk value after about three to seven periods, depending on the bulk composition. This is consistent with the formation of a layered structure of spherical micelles induced by the surface.

Similar observations were reported from aqueous dispersions of silica particles by Madsen *et al* [119]. Solutions with a colloid volume fraction of $\phi \approx 0.27$, i.e. roughly half the value required for bulk crystallization of a hard sphere suspension, were investigated by applying XR and GIXD. The observed electron density profiles showed undulations with a period which coincides roughly with the particle diameter. On the other hand, no diffraction peaks could be detected in GIXD. Therefore it is assumed that the particles arrange in layers which, however, do not have any lateral order.

Very recently, Lang *et al* reported an investigation on the isotropic to nematic transition of thread-like blockcopolymer micelles close to a solid wall [120]. They find the formation of a nematic layer adjacent to the wall at a volume fraction which is roughly 85% of the volume fraction required to induce the nematic phase in the bulk. This is in qualitative agreement with theoretical prediction and simulations for hard rod suspensions by van Roij *et al* and Dijkstra *et al* [121, 122]. However, the thickness of the observed nematic layer was not in the range of the thread contour length, as to be expected from the theoretical prediction, but rather in the range of the threads persistence length. The latter finding is in good agreement with the theoretical predictions by Chen *et al* which take into account the finite flexibility of the micelles [123, 124].

6. Conclusions

To summarize, we have collected experimental reports and some theoretical as well as computer simulation approaches on surface ordering phenomena in soft condensed matter systems. The broadest experimental basis clearly exists for melts of linear chain molecules. The variety of surface phase behaviour and structural properties increases rapidly with the complexity of molecular interactions and shape. A quantitative microscopic theory based on experimental knowledge of the molecular interaction is still not available. On the other hand, this kind of theory is available for colloidal suspensions, as in these cases the pair interaction potentials are often sufficiently simple to allow for a thorough microscopic description. Further, surface ordering effects in colloidal suspensions have gained increasing interest from experimentalists over the last decade, and we are therefore confident that further experimental investigations in this field will promote our understanding of these effects in general.

Acknowledgments

References

[1] Ninham B W 1999 *Adv. Colloid Interface Sci.* **83** 1
[2] Penfold J 2001 *Rep. Prog. Phys.* **64** 777
[3] Frenken J W M and van der Veen F F 1985 *Phys. Rev. Lett.* **54** 134
[4] Regan M J, Kawamoto E H, Lee S, Pershan P S, Maskil N, Deutsch M, Magnussen O M, Ocko B M and Berman L E 1995 *Phys. Rev. Lett.* **75** 2498
[5] Regan M J, Pershan P S, Magnussen O M, Ocko B M, Deutsch M and Berman L E 1996 *Phys. Rev.* B **54** 9730

[6] Regan M J, Tostmann H, Pershan P S, Magnussen O M, DiMasi E, Ocko B M and Deutsch M 1997 *Phys. Rev.* B **55** 10786
[7] Ercolessi F, Di Tolla F D and Tosatti E 1997 *Surf. Rev. Lett.* **4** 833
[8] Celestini F, Ercolessi F and Tosatti E 1997 *Surf. Sci.* **377** 914
[9] Tostmann H, DiMasi E, Pershan P S, Ocko B M, Shpyrko O G and Deutsch M 1997 *Phys. Rev.* B **59** 783
[10] Turchanin A, Freyland W and Nattland D 2002 *Phys. Chem. Chem. Phys.* **4** 647
[11] Kroes G J 1992 *Surf. Sci.* **275** 365
[12] Elbaum M, Lipson S G and Dash J G 1993 *J. Cryst. Growth* **129** 491
[13] Lied A, Dosch H and Bilgram J H 1994 *Phys. Rev. Lett.* **72** 3554
[14] Lied A, Dosch H and Bilgram J H 1994 *Physica* B **198** 92
[15] Dosch H, Lied A and Bilgram J H 1995 *Surf. Sci.* **327** 145
[16] Dosch H, Lied A and Bilgram J H 1996 *Surf. Sci.* **366** 43
[17] Furukawa J and Nada H 1997 *J. Phys. Chem.* B **101** 6167
[18] Makkonen L 1997 *J. Phys. Chem.* B **101** 6196
[19] Wilson P W, Arthur J W and Haymet A D J 1999 *Biophys. J.* **77** 2850
[20] Maruyama M, Sato T, Taniguchi S, Kawamura M, Kodera S, Kishimoto Y and Furukawa Y 2000 *Japan. J. Appl. Phys.* **39** 6696
[21] Doppelschmidt A and Butt H J 2000 *Langmuir* **16** 6709
[22] Wei X, Miranda P B and Shen Y R 2001 *Phys. Rev. Lett.* **56** 1554
[23] Wei X, Miranda P B, Zhang C and Shen Y R 2002 *Phys. Rev.* B **66** 085401
[24] Sadtchenko V and Ewing G E 2003 *Can. J. Phys.* **81** 333
[25] Suzanne J, Ferry D, Demirdjan B, Girardet C, Toubin C, Picaud S and Hoang P N M 2003 *Can. J. Phys.* **81** 415
[26] Magnussen O M, Ocko B M, Regan M J, Penanen K, Pershan P S and Deutsch M 1995 *Phys. Rev. Lett.* **74** 4444
[27] Miyano K 1979 *Phys. Rev. Lett.* **43** 51
[28] Miyano K 1979 *J. Chem. Phys.* **71** 4108
[29] Als-Nielsen J, Christensen F and Pershan P S 1982 *Phys. Rev. Lett.* **48** 1107
[30] Pershan P S and Als-Nielsen J 1984 *Phys. Rev. Lett.* **52** 759
[31] Lucht R and Bahr Ch 1997 *Phys. Rev. Lett.* **78** 3487
[32] Lucht R, Bahr Ch, Heppke G and Goodby J W 1998 *J. Chem. Phys.* **108** 3716
[33] Schadt M and Helfrich W 1970 *Appl. Phys. Lett.* **18** 127
[34] Kappl M and Butt H J 2002 *Part. Part. Syst. Charact.* **19** 129
[35] Prieve D C 1999 *Adv. Colloid Interface Sci.* **82** 93
[36] Claesson P M, Ederth T, Bergeron V and Rutland M W 1996 *Adv. Colloid Interface Sci.* **67** 119
[37] Warren B E 1990 *X-ray Diffraction* (New York: Dover)
[38] Marra W C, Eisenberger P and Cho A Y 1979 *J. Appl. Phys.* **50** 6927
[39] Eisenberger P and Marra W C 1981 *Phys. Rev. Lett.* **46** 1081
[40] For a brief introduction see Kjær C 1994 *Physica* B **198** 100
[41] For an overview see Als-Nielsen J, Kjær C, Leveiller F, Lahav M and Leiserowitz L 1994 *Phys. Rep.* **246** 251
[42] Parratt L G 1954 *Phys. Rev.* **95** 359
[43] Lang P 1999 Amphiphiles at interfaces studied by surface sensitive x-ray scattering *Modern Characterization Methods of Surfactant Systems* (*Surfactant Science Series* vol 83) ed B P Binks (New York: Dekker) pp 375–413
[44] Fischer D 1954 *PhD Thesis* Technische Hochschule Karlsruhe, Germany
[45] Gang H, Patel J, Wu X Z, Deutsch M, Gang O, Ocko B M and Sirota E B 1998 *Europhys. Lett.* **43** 314
[46] Earnshaw J C and Hughes C J 1992 *Phys. Rev.* A **46** 4494
[47] Wu X Z, Sirota E B, Sinha S K, Ocko B M and Deutsch M 1993 *Phys. Rev. Lett.* **70** 958
[48] Wu X Z, Ocko B M, Sirota E B, Sinha S K, Deutsch M, Cao B H and Kim M W 1993 *Science* **261** 1018
[49] Wu X Z, Ocko B M, Sirota E B, Sinha S K and Deutsch M 1993 *Physica* A **200** 751
[50] Ocko B M, Wu X Z, Sirota E B, Sinha S K, Gang O and Deutsch M 1997 *Phys. Rev.* E **55** 3164
[51] Pfohl T, Beaglehole D and Riegler H 1996 *Chem. Phys. Lett.* **260** 82
[52] Maeda N, Kohonen M H and Christenson H K 1999 *Phys. Rev.* E **61** 7239
[53] Maeda N, Kohonen M H and Christenson H K 2001 *J. Phys. Chem.* B **105** 5906
[54] Yamamoto Y, Ohara H, Kajikawa K, Ishii H, Ueno N, Seki K and Ouch Y 1999 *J. Electron. Spectrosc. Relat. Phenom.* **101** 555
[55] Merkl C, Pfohl T and Riegler H 1997 *Phys. Rev. Lett.* **79** 4625
[56] Holzwarth A, Leporatti S and Riegler H 2000 *Europhys. Lett.* **52** 653

[57] Schollmeyer H, Struth B and Riegler H 2003 *Langmuir* **19** 5042
[58] Volkmann U G, Pino M, Altamirano L A, Taub H and Hansen F Y 2002 *J. Chem. Phys.* **116** 2107
[59] Kern H, Rybinski W v and Findenegg G H 1977 *J. Colloid Interface Sci.* **59** 301
[60] Grosse-Rhode M and Findenegg G H 1978 *J. Colloid Interface Sci.* **64** 374
[61] Weckesser J, Fuhrmann D, Weiss K, Wöll C and Richardson N V 1997 *Surf. Rev. Lett.* **4** 209
[62] Wu Z, Ehrlich S N, Matthies B, Herwig K W, Pengcheng D, Volkmann U G, Hansen F Y and Taub H 2001 *Chem. Phys. Lett.* **348** 168
[63] Yeganeh M S 2002 *Phys. Rev.* E **66** 041607
[64] Leermakers F A M and Cohen-Stuart M A 1995 *Phys. Rev. Lett.* **76** 82
[65] Sirota E B, Wu X Z, Ocko B M and Deutsch M 1997 *Phys. Rev. Lett.* **79** 531
[66] Tkachenko A V and Rabin Y 1996 *Phys. Rev. Lett.* **76** 2527
[67] Tkachenko A V and Rabin Y 1997 *Phys. Rev.* E **55** 778
[68] Tkachenko A V and Rabin Y 1997 *Phys. Rev. Lett.* **79** 532
[69] Li H Z and Yamamoto T 2001 *J. Chem. Phys.* **114** 5774
[70] Li H Z and Yamamoto T 2002 *J. Phys. Soc. Japan* **71** 1083
[71] Shimizu T and Ymamoto T 2000 *J. Chem. Phys.* **113** 3351
[72] Xia T K and Landmann U 1993 *Phys. Rev.* B **48** 11313
[73] Smith P, Lynden-Bell R M, Earnshaw J C and Smith W 1999 *Mol. Phys.* **96** 249
[74] Gang H, Gang O, Shao H H, Wu X Z, Patel J, Hsu C S, Deutsch M, Ocko B M and Sirota E B 1998 *J. Phys. Chem.* B **102** 2754
[75] Deutsch M, Wu X Z, Sirota E B, Sinha S H, Ocko B M and Magnussen O M 1995 *Europhys. Lett.* **30** 283
[76] Gang O, Ocko B M, Wu X Z, Sirota E B and Deutsch M 1998 *Phys. Rev. Lett.* **80** 1264
[77] Gang O, Wu X Z, Ocko B M, Sirota E B and Deutsch M 1998 *Phys. Rev.* E **58** 6086
[78] Wang J L, Leveiller F, Jacquemain D, Kjær C, Als-Nielsen J, Lahav M and Leiserowitz L 1994 *J. Am. Chem. Soc.* **116** 1192
[79] Binks B P, Fletcher P D I, Kotsev S N and Thompson R L 1997 *Langmuir* **13** 6669
[80] Gang O, Ellmann J, Möller M, Kraack H, Sirota E B, Ocko B M and Deutsch M 2000 *Europhys. Lett.* **49** 761
[81] Marczuk P and Lang P 1998 *Macromolecules* **31** 9013
[82] Wu X Z, Ocko B M, Tang H, Sirota E B, Sinha S K and Deutsch M 1995 *Phys. Rev. Lett.* **75** 1332
[83] Wu X Z, Ocko B M, Deutsch M, Sirota E B and Sinha S K 1996 *Physica* B **221** 261
[84] Sloutskin E, Sirota E B, Kraack H, Ocko B M and Deutsch M 2001 *Phys. Rev.* E **64** 031708
[85] Doerr A, Wu X Z, Ocko B M, Sirota E B, Gang O and Deutsch M 1997 *Colloids Surf.* A **128** 63
[86] Sloutskin E, Sirota E B, Kraack H, Gang O, Doerr A, Ocko B M and Deutsch M 2002 *J. Chem. Phys.* **116** 8056
[87] Gang O, Ocko B M, Wu X Z, Sirota E B and Deutsch M 1999 *Phys. Rev. Lett.* **82** 588
[88] Gang O, Ocko B M, Wu X Z, Sirota E B and Deutsch M 2000 *Colloids Surf.* A **164** 55
[89] Gang O, Ocko B M, Wu X Z, Sirota E B and Deutsch M 2000 *J. Phys.: Condens. Matter* **12** A357
[90] Sloutskin E, Kraack H, Gang O, Ocko B M, Sirota E B and Deutsch M 2003 *J. Chem. Phys.* **118** 10729
[91] Sloutskin E, Wu X Z, Peterson T B, Gang O, Ocko B M, Sirota E B and Deutsch M 2003 *Phys. Rev.* E **68** 031605
[92] Sloutskin E, Gang O, Kraack H, Doerr A, Sirota E B, Ocko B M and Deutsch M 2003 *Phys. Rev.* E **68** 031606
[93] Binks B P, Fletcher P D I, Sager W F C and Thompson R L 1995 *Langmuir* **11** 977
[94] Binks B P, Fletcher P D I and Thompson R L 1996 *Ber. Bunsenges. Phys. Chem.* **100** 232
[95] Hayami Y and Findenegg G H 1997 *Langmuir* **13** 4865
[96] Marczuk P, Lang P, Findenegg G H, Mehta S K and Möller M 2002 *Langmuir* **18** 6830
[97] Pieranski P 1980 *Phys. Rev. Lett.* **45** 569
[98] Zahn K, Lenke R and Maret G 1999 *Phys. Rev. Lett.* **82** 2721
[99] van Blaaderen A, Ruel R and Wiltzius P 1997 *Nature* **385** 321
[100] Heni M and Löwen H 2001 *J. Phys.: Condens. Matter* **13** 4675
[101] Luzatti V, Mustacci H, Skoulios A and Hussan F 1960 *Acta Cryst.* **13** 660
[102] Mitchell D J, Tiddy G J T, Waring L, Bostock T and MacDonald M P 1983 *J. Chem. Soc. Faraday Trans.* I **79** 975
[103] Sjöblom J, Stenius P and Danielsson I 1997 Phase equilibria of nonionic surfactants and the formation of microemulsions *Nonionic Surfactants Physical Chemistry* (*Surfactant Science Series* vol 23) ed M Schick (New York: Dekker) pp 369–434
[104] Won Y Y, Davis H T and Bates F S 1999 *Science* **283** 960
[105] Alexandridis P and Lindman B 2000 *Amphiphilic Block Copolymers: Self-Assembly and Application* (New York: Elsevier)

[106] Schwartz D K, Braslau A, Ocko B M, Pershan P S, Als-Nielsen J and Huang J S 1988 *Phys. Rev.* A **38** 5817
[107] Chou C H, Regan M J, Pershan P S and Zhou L 1997 *Phys. Rev.* E **55** 7212
[108] Strey R, Schomäcker R, Roux D, Nallet F and Olsson U 1990 *J. Chem. Soc. Faraday Trans.* I **86** 2253
[109] Braun C, Lang P and Findenegg G H 1995 *Langmuir* **11** 764
[110] Lang P, Braun Chr, Steitz R, Findenegg G H and Rhan H 1998 *J. Phys. Chem.* B **102** 7590
[111] Lang P 1999 *J. Phys. Chem.* B **103** 5100
[112] Lang P, Steitz R and Braun Chr 2000 *Colloids Surf.* A **163** 91
[113] Bolhuis P, Hagen M and Frenkel D 1994 *Phys. Rev.* E **50** 4880
[114] Courtemanche D J and van Swol F 1992 *Phys. Rev. Lett.* **69** 2078
[115] Courtemanche D J, Pasmore T A and van Swol F 1993 *Mol. Phys.* **80** 861
[116] Gerstenberg M C, Pedersen J S and Smith G S 1998 *Phys. Rev.* E **58** 8028
[117] Gerstenberg M C and Pedersen J S 2001 *Langmuir* **17** 7040
[118] Gerstenberg M C, Pedersen J S, Majewski J and Smith G S 2002 *Langmuir* **18** 4933
[119] Madsen A, Konovalov O, Robert A and Grübel G 2001 *Phys. Rev.* E **64** 061406
[120] Lang P, Willner L, Pyckhout-Hintzen W and Krastev R 2003 *Langmuir* **19** 7597
[121] van Roij R, Dijkstra M and Evans R 2000 *J. Chem. Phys.* **113** 7689
[122] Dijkstra M, van Roij R and Evans R 2001 *Phys. Rev.* E **63** 1703
[123] Cui S M, Akcakir O and Chen Z Y 1995 *Phys. Rev.* E **51** 4548
[124] Chen Z Y and Cui S M 1995 *Phys. Rev.* E **52** 3876